Case Studies in Thermal Engineering 54 (2024) 104045

Contents lists available at ScienceDirect

Case Studies in Thermal Engineering

journal homepage: www.elsevier.com/locate/csite

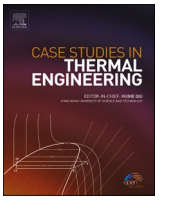

Experimental investigation of air-conditioning electrical compressor using binary TiO_2–SiO_2 polyol-ester nanolubricants

N.N.M. Zawawi [a], W.H. Azmi [a,b,*], A.H. Hamisa [b,c], Tri Yuni Hendrawati [d], A.R.M. Aminullah [b]

[a] Centre for Research in Advanced Fluid and Processes, Lebuhraya Tun Razak, 26300, Gambang, Kuantan, Pahang, Malaysia
[b] Faculty of Mechanical and Automotive Engineering Technology, Universiti Malaysia Pahang Al-Sultan Abdullah, 26600, Pekan, Pahang, Malaysia
[c] Faculty of Science, Engineering and Agrotechnology, University College of Yayasan Pahang, 25050, Kuantan, Pahang, Malaysia
[d] Department of Chemical Engineering, Universitas Muhammadiyah Jakarta, Jl. Cempaka Putih Tengah 27, Jakarta, 10510, Indonesia

ARTICLE INFO

Handling Editor: Huihe Qiu

Keywords:
Nanolubricant
Polyol-ester
Refrigeration system
Electric compressor
Hybrid vehicle

ABSTRACT

As electric vehicles (EVs) continue to replace conventional gasoline vehicles, maintaining thermal comfort within the car requires additional energy to operate the automotive air-conditioning (AAC) system. This work aims to optimise the electrically driven compressor (EDC) system utilising polyol-ester (POE)-based binary nanolubricants to enhance performance and minimise the size of the EV battery and AAC components. A binary nanolubricant was formulated using a two-step method of formulation. The TiO_2–SiO_2/POE binary nanolubricant was prepared at different volume concentrations ranging from 0.01 to 0.1 %. The experiment was conducted for the 1200–3840 rpm compressor speed with different initial refrigerant charges between 120 and 160 g. The heat absorption rose by up to 44.2 % while utilising the binary nanolubricant at a volume concentration of 0.03 %. The coefficient of performance (COP) reached its maximum value of 2.43 at a refrigerant charge of 160 g and compressor speed of 1860 rpm. Furthermore, the binary nanolubricant significantly reduced the expansion valve discharge temperature, exhibiting a substantial decrease of up to 51.6 %. The highest COP increment, up to 23.4 %, was achieved at a volume concentration of 0.03 %. Hence, it is recommended to utilise 0.03 % TiO_2–SiO_2/POE binary nanolubricant to achieve optimal performance in the AAC-EDC system.

Nomenclature

AAC	automobile air-conditioning
BDE	belting-driven compressor
BHT	butylated hydroxytoluene
COP	coefficient of performance
cSt	centistokes
EDC	electrically-driven compressor
EDX	energy dispersive X-ray
EEV	efficient energy vehicles

* Corresponding author. Centre for Research in Advanced Fluid and Processes, Lebuhraya Tun Razak, 26300, Gambang, Kuantan, Pahang, Malaysia.
E-mail addresses: naal30@gmail.com (N.N.M. Zawawi), wanazmi@umpsa.edu.my (W.H. Azmi), hamisa@ucyp.edu.my (A.H. Hamisa), yuni.hendrawati@umj.ac.id (T.Y. Hendrawati), maminullah@tatiuc.edu.my (A.R.M. Aminullah).

https://doi.org/10.1016/j.csite.2024.104045
Received 19 October 2023; Received in revised form 8 January 2024; Accepted 18 January 2024
Available online 19 January 2024

h	enthalpy
EV	electric vehicles
HFC	hydrofluorocarbon
m	mass, g
N	compressor speed, rpm
P	pressure, kPa
PAG	polyalkylene glycol
POE	polyol-ester
P_{USAGE}	power consumption, W
PWM	pulse width modulation
Q_L	heat absorption, kJ/kg
$\dot{Q}_L$	cooling capacity, kJ/kg
RSE	relative standard error
T	temperature, °C
TEM	transmission electron microscopy
VCRS	vapour compression refrigeration system
W_{in}	compressor work, kJ/kg

Greek symbols

φ	volume concentration, %
μ	dynamic viscosity, cSt
ρ	density, kg/m^3

Subscripts

L	lubricant
p	nanoparticle

1. Introduction

The most energy-intensive auxiliary component in both conventional and hybrid electric vehicles is the AAC system [1]. The system is also the second-largest energy source in automobiles [2], behind the power train [3]. The air conditioning system in conventional vehicles is powered by a compressor driven by a belt (AAC-BDC). On the other hand, air conditioning system in the EVs uses an electrically driven compressor (AAC-EDC), which derives power from the vehicle's battery. The AAC-EDC system performances must be enhanced to eliminate environmental impact and reduce reliance on global fuel use. Government policies, acts, and laws on energy conservation have been implemented in several nations worldwide to reduce energy usage, costs, and greenhouse gas emissions. The EVs appear to be one of the best answers to energy and climate change issues and have the advantages of zero emissions and zero fuel consumption [4].

Due to the growing concern over energy prices, thermal comfort, greenhouse gas emissions, and the manufacture of efficient energy vehicles (EEV), an efficient AAC system is urgently needed today. The technological advancement of vapour compression (VCRS) can enhance the performance and reduce the workload of the automotive engine [5–9]. Adding an electrically powered system to the AAC can reduce fuel consumption while enhancing engine performance [10–13]. The need for an effective AAC system in EEV becomes a demand for auto manufacturers to optimise energy efficiency and improve overall performance. Powering the auxiliary AAC and EDC system is a considerable difficulty for the EV propulsion system. The EVs are propelled solely by the electrical energy contained in their battery pack. Despite its compact design, the AAC-EDC system consumes more power, which could harm the vehicle's overall performance and increase the battery's size, weight, volume, and cost.

The early works on the EDC for refrigeration systems were undertaken by Sendil and Elansezhian [14], Sendil and Elansezhian [15], Subramani and Prakash [16] and Sabareesh et al. [17]. However, instead of using the AAC-EDC system, the authors applied VCRS with a hermetic compressor for residential refrigerators [18–20]. Additionally, some parts and tube lines from the automobile parts were not considered. Therefore, it is necessary to start new research on AAC-EDC systems using an entire automobile component (including the compressor). The most recent advancement of the AAC system with nanolubricants was accomplished; however, it is limited to the AAC-BDC system [21].

The compressors of AAC systems can potentially be improved by using nanoparticle dispersion technology in conjunction with nanolubricants [22–25]. While studies have examined the efficacy of nanolubricants in the AAC system, with most focusing on butylated hydroxytoluene (BHT) and polyalkylene-glycol (PAG) nanolubricants [26,27], insufficient research has been carried out on the implementation of AAC-EDC systems utilising POE lubricant or nanolubricants. The use of nanoparticles as additives of lubricants in the AAC-EDC system will possibly boost its performance, thereby reducing the size of both the battery and AAC components. Krishnan et al. [28] conducted relevant research on POE-based nanolubricants, demonstrating the marked improvement in the VCRS performance with nanoparticle dispersion in POE lubricants [29–31]. Although Redhwan et al. [32] and Hamisa et al. [33] studied nanolubricants' application in AAC-BDC systems, no efforts have been documented in the literature on utilising nanolubricants in

Table 1
Properties of SiO_2 and TiO_2 nanoparticles [37,38].

Property	SiO_2	TiO_2
Thermal Conductivity (W/m K)	1.4	8.4
Specific heat (J/kg K)	745	692
Density, kg/m^3 @ 20 °C	2220	4230

Table 2
Properties of POE RL68H lubricant [39].

Property	POE RL68H
Viscosity @ 40 °C (cSt)	66.6
Viscosity @ 100 °C (cSt)	9.4
Pour Point (°C)	−39
Density @ 20 °C (g/ml)	0.977
Flash Point COC (°C)	270

AAC-EDC systems.

Sharif et al. [34] studied the implementation of SiO_2/PAG nanolubricants in the AAC system. They reported a considerable enhancement in the COP by up to 24 %, with an average increase of 10.5 %. Redhwan et al. [35] explored using Al_2O_3/PAG nanolubricants in the AAC system and observed improved COP, reduced compressor work, and increased cooling capacity at a 0.01 % volume concentration of Al_2O_3/PAG nanolubricants. The use of mono nanolubricants is subject to certain constraints related to stability, compressor work, wear rates, and AAC system performance. Hence, AAC performance continued to be investigated by Zawawi et al. [26] using Al_2O_3–SiO_2/PAG binary nanolubricants with a composition ratio 60:40 at 0.015 % volume concentrations. COP enhancements up to 28.10 % were reported at volume concentrations of 0.015 % for the binary nanolubricants. The study provides evidence that utilising binary nanolubricants can significantly improve the performance of binary nanolubricants and enhance the AAC system's performance. Using binary nanolubricants within the air conditioning system is anticipated to result in an elevation of the COP and a corresponding decrease in compressor work [36]. However, it is worth noting that these studies were limited to PAG-based nanolubricants and AAC-BDC systems.

This study will evaluate binary nanolubricants regarding the AAC-EDC system's cooling capacity, expansion valve discharge temperature and power consumption. Specifically, TiO_2–SiO_2/POE nanolubricants will be utilised, prepared by a two-step method, and examined for stability. Test benches are developed for analysing the performance of the AAC-EDC system. An experimental investigation is then carried out using TiO_2–SiO_2/POE binary nanolubricants to gather data that supports the use of nanolubricants in the system. Furthermore, the study examines the effects of TiO_2–SiO_2/POE binary nanolubricants on the performance of the AAC-EDC system to find the optimal volume concentration of these nanolubricants.

2. Characterisation of POE-based binary nanolubricants

2.1. Materials properties

Nanoparticles of metal oxides, specifically SiO_2 and TiO_2, were employed to create nanolubricants, and their properties were detailed in Table 1 using Energy Dispersive X-ray (EDX) analysis. In addition, Transmission Electron Microscopy (TEM) was also utilised to characterise these nanoparticles further. The EDC lubricant for the AAC-EDC system was selected to be the polyol-ester (POE) lubricant. Table 2 highlights the properties of an ISO VG 68 synthetic POE lubricant, which enhances the system's durability and functionality by providing exceptional wear protection for steel and aluminium surfaces. Its wide range of applicability stems from its low-temperature characteristics and high thermal and chemical stability.

TiO_2 and SiO_2 nanoparticles have amorphous and anatase crystal structures, respectively. The chemical stability, heat resistance, durability, and non-toxic particles of anatase TiO_2 are well recognized [40]. TiO_2 is a good heat transfer material since it is stable, accessible, affordable, and environmentally safe [41]. SiO_2 nanoparticles, among other types of nanoparticles, are frequently used to combine and mix with other types of nanoparticles, such as SiO_2–TiO_2, SiO_2–Al_2O_3, and SiO_2-CNT nanoparticles [42–45]. Silicon is the second most common element in the earth's crust after oxygen; constant use would not deplete it [46]. In addition to being produced cheaply, silica nanoparticles are believed to be the safest non-toxic particles for drug delivery and DNA conjugation because they are hydrophilic, have a large specific surface area, and are well biocompatible [47]. Due to its advantages in various fields like surface engineering [48], pharmaceuticals [49], oilfield operation [45], and drug delivery [50], silicon oxide (SiO_2) nanoparticles are frequently used for heat transfer applications.

2.2. Nanolubricants preparation

Each sample contained 100 ml of nanolubricants for use in the EDC compressor and was produced using a two-step method, with concentration ranges of up to 0.1 %. The mass of the nanoparticles at a particular volume concentration was calculated using Equation (1);

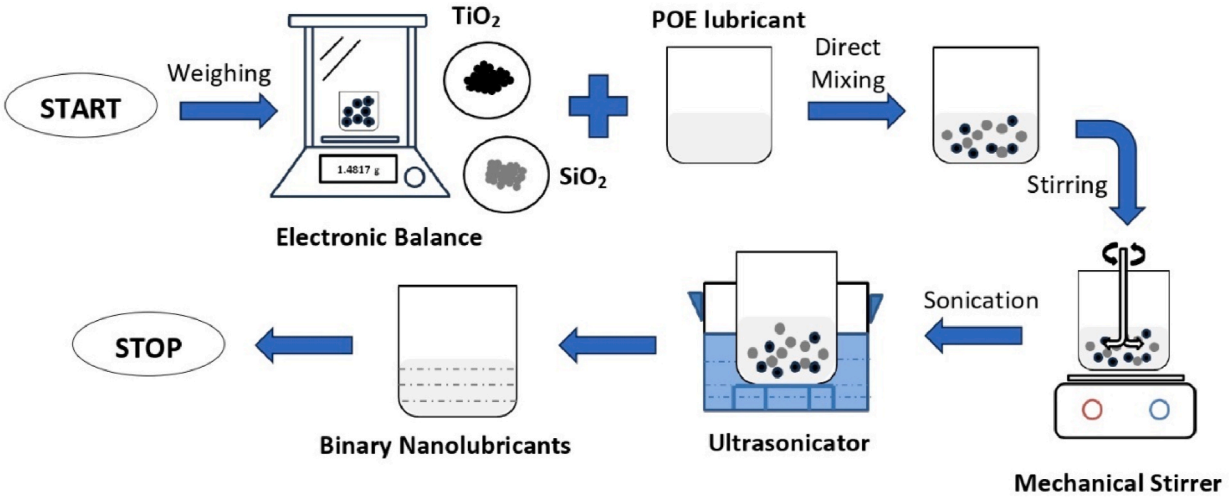

Fig. 1. Preparation of binary nanolubricant via the application of a two-step method.

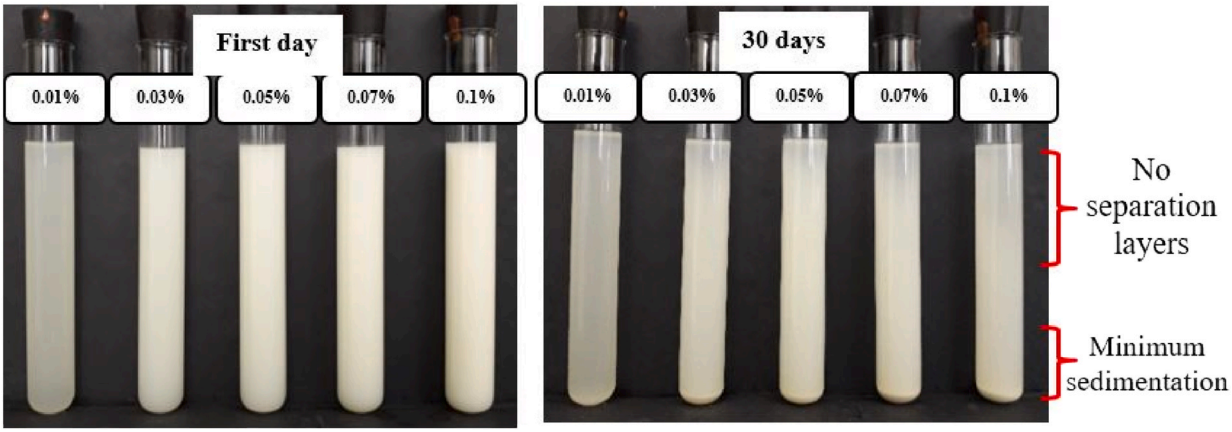

Fig. 2. Visual sedimentation for TiO_2–SiO_2/POE nanolubricants.

$$\varphi = \frac{m_p/\rho_p}{m_p/\rho_p + m_l/\rho_l} \times 100\% \tag{1}$$

where m_p and m_L are the nanoparticle and lubricant masses, respectively, φ is the concentration in volume percent, with ρ_p and ρ_L are the nanoparticle and lubricant density, respectively. The mechanical agitation process lasted approximately 30 min at room temperature. Using a Fisherbrand FB15015 ultrasonic bath vibrator, the nanolubricant was then homogenised continuously while being stirred and agitated. The ultrasonic bath vibrator homogeniser produces ultrasonic pulses with a 50 kHz frequency. The bath frequency, water temperature, and volume are held constant throughout the sonication procedure. Fig. 1 depicts the two-step process for preparing TiO_2–SiO_2/POE binary nanolubricant.

2.3. Nanolubricants stability

Before beginning the ultrasonication procedure, the optimum sonication time for the nanolubricant was analysed. Five samples of nanolubricant at a concentration of 0.05 % by volume were initially created with varying sonication periods ranging from zero to 2 h at half-hour intervals and increasing to 6 h at 2-h intervals. An Ultraviolet–visible (UV–Vis) spectrophotometer was then applied to determine the appropriate sonication time. The nanolubricant sonicated for 3 h without adding surfactant performed the best. Several methods were used to evaluate stability: the photographic sedimentation technique, UV–Vis analysis, micrograph assessment using Transmission electron microscopy (TEM), and zeta potential testing.

The TiO_2–SiO_2/POE binary nanolubricant was left undisturbed in test tubes for up to 30 days while maintained at varying volume concentrations. Daily monitoring was conducted on the samples, and images were captured on the first day of preparation and again after 30 days for qualitative comparative analysis. Fig. 2 illustrates the binary nanolubricant samples with varying volume concentrations. The observed stability of the binary nanolubricant was consistent with the findings reported by Zawawi et al. [26]. The

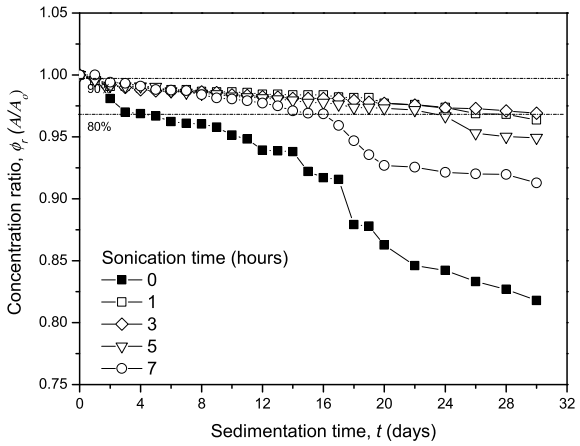

Fig. 3. Concentration ratio of TiO_2–SiO_2/POE nanolubricants at different sonication time.

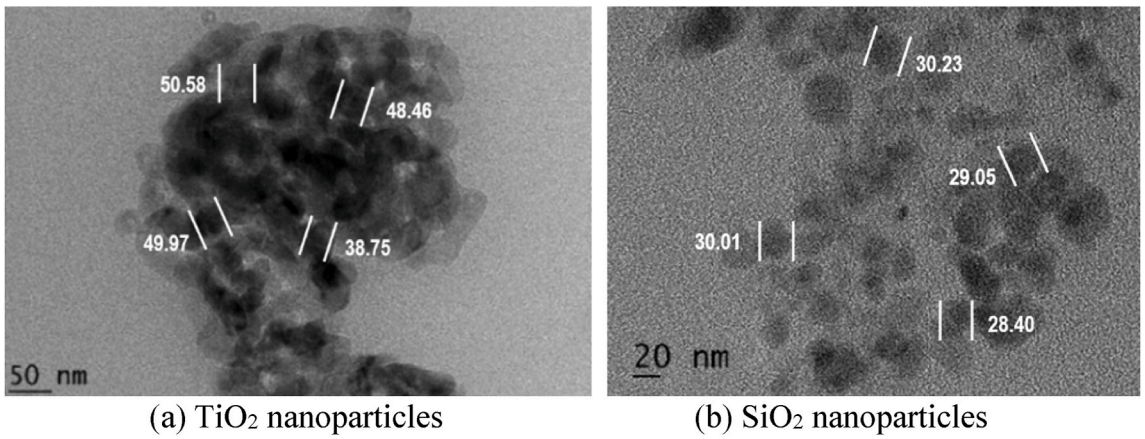

(a) TiO_2 nanoparticles (b) SiO_2 nanoparticles

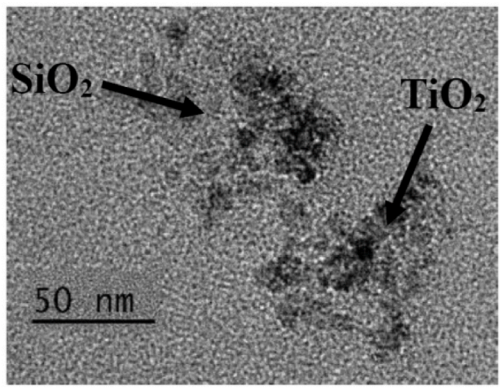

(c) TiO_2-SiO_2/POE nanolubricants

Fig. 4. TEM images TiO_2–SiO_2/POE binary nanolubricants (a) TiO_2 nanoparticles (b) SiO_2 nanoparticles (c)TiO_2–SiO_2/POE nanolubricants.

utilisation of a composite of two distinct nanoparticles functioned as an additive, synergistically enhancing the dispersion properties, and contributing to preserving the exceptional stability of the POE lubricants. The stability of TiO_2–SiO_2/POE binary nanolubricants, which incorporate SiO_2 and TiO_2 nanoparticles, was enhanced.

Fig. 3 shows the concentration ratio versus sedimentation time at different sonication times for TiO_2–SiO_2/POE nanolubricants. According to the observations, it has been determined that all sonication time samples exhibit the ability to retain over 90 % of their initial volume concentration for 30 days. The control sample without sonication drops to 82 % after 30 days. Based on the results, 3 h of

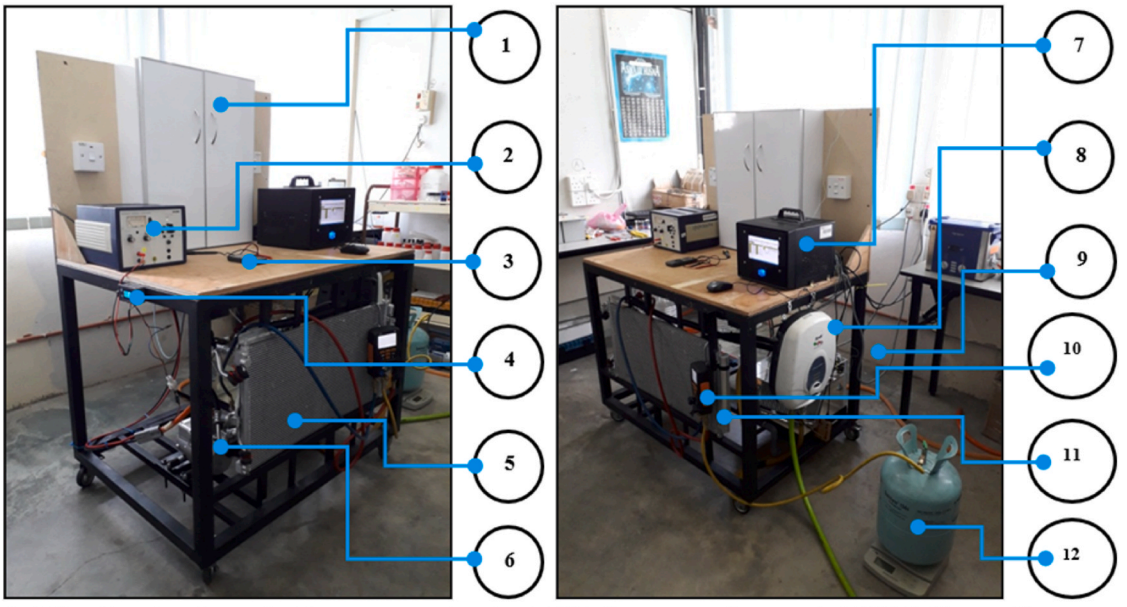

1. Distribution box, 2. Power supply, 3. AC/DC power clamp, 4. PWM Controller, 5. Condenser, 6. Electrically-driven compressor (EDC), 7. Data logger module, 8. Water heater, 9. Evaporator inside water bath, 10. Digital Pressure Gauge, 11. Receiver Dryer, 12. R134a refrigerant and weight scale

(a) Experimental Setup

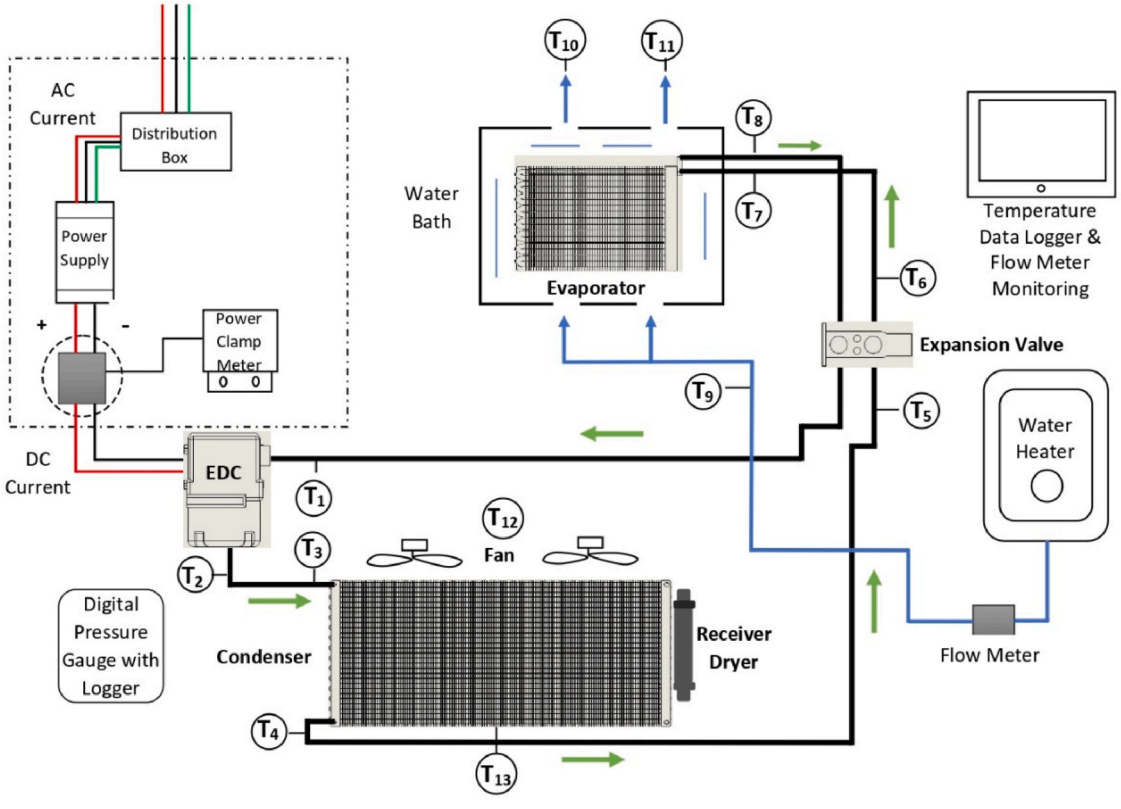

(b) Schematic Diagram

(caption on next page)

Fig. 5. AAC-EDC system experimental setup (a) Experimental Setup (b) Schematic Diagram.

sonication time was chosen as the optimal time for binary nanolubricants with a concentration of up to 0.97, higher than the other four samples. The stability of nanoparticles is adversely affected by prolonged sonication, particularly when the suspension has a limited volume concentration range [51]. This behaviour can result in harmful effects and significant breakdown of the nanoparticles. Therefore, preparing binary TiO_2–SiO_2/POE nanolubricant at various concentrations up to 0.1 % is considered for 3 h of sonication time only and it is sufficient to sustain the stability for a longer period.

The present study utilises TEM to examine the distribution state of nanoparticles suspended in POE lubricants. The TEM imaging technique was used to confirm the size, arrangement, and aggregation of the two nanoparticles after they were mixed with POE lubricants and used in the experiments conducted by other researchers. For the evaluation and confirmation of the particle radius of suspended hybrid nanoparticles in the POE lubricants, an approach was implemented to analyse TEM images utilising the image analysis tool Image J. Fig. 4 shows the particle distribution of TiO_2 and SiO_2 nanoparticles in binary nanolubricant on the TEM images. The image shows TiO_2 and SiO_2 nanoparticles have good and uniform dispersion with lesser agglomeration while suspended in the lubricant. It was determined that the TiO_2–SiO_2/POE nanolubricants had a zeta potential value of 276.8 mV, which exceeded the stability limit of 60 mV, confirming that the nanolubricants were in excellent colloidal condition.

3. Automotive air conditioning with AAC-EDC system

3.1. Experimental setup

Using the original components of the AAC system for EV, an experimental setup was developed to evaluate the efficiency of the AAC system with a new lubricant. The configuration of the AAC-EDC system setup is illustrated in Fig. 5 [52]. The design comprises the refrigeration system consisting of the car's AAC system, including the EDC, condenser, expansion valve, receiver dryer, and evaporator. The AAC system featured a scroll-type EDC compressor and was powered by a 12 V DC EDC with a maximum output of 700 W. Compressor speed was controlled using a pulse width modulation (PWM) controller, which varied the speed between 1200 and 4500 rpm. A cycling system was installed to prevent the compressor from running continuously during the experiment. The expansion valve is utilised to expand refrigerant in the air AAC system. The thermal expansion valve can adjust the refrigerant flow in response to environmental conditions by increasing or decreasing it as required. The AAC system equipped with an expansion valve exhibits enhanced efficiency, a more comprehensive temperature range, and an expanded refrigerant charge range compared to a capillary tube system. In contrast, the capillary tube is the throttling device in domestic refrigerators, deep freezers, water coolers, and residential air conditioners.

In addition, the test rig included a water bath for the evaporator, an inverter frequency controller, a data logger, piping systems, and measurement instruments. The system's cooling capacity was determined using the ASHRAE 41.9–2000 standard [53] by submerging the evaporator in a water bath. Water bath systems included flow transducers, two-way inlet and outlet pipes, and insulated tanks that controlled water temperature and flow rate with a water heater. Temperature indicators, pressure gauges, and flow-rate sensors were appropriately installed in the AAC-EDC system. The temperatures at these points were measured using a calibrated K-type thermocouple in line with the ANSI/ASHRAE (1986) standard. The data logger module tracked and recorded each water flow rate and temperature measurement. A calibrated digital gauge was used to measure and record the evaporator and condenser pressures. Using AC/DC power clamps, the system's power consumption was manually measured, monitored, and recorded. The performance of automotive air conditioning systems is significantly influenced by external ambient conditions, including temperature and relative humidity. In this experiment, the ambient temperature was fixed at constant 25 °C and relative humidity 55 %. Consequently, an environmental chamber was created to regulate the ambient temperature and humidity. The controlled ambient temperature range deemed acceptable was between 24.5 and 25.5 °C. Similarly, the acceptable range for relative humidity was between 45 % and 65 %, to comply the SAEJ2765 [54].

3.2. Experimental procedure

Before the experiment, the AAC-EDC test rig was filled with R134a at a pressure of 300 kPa. This pressure was maintained for 24 h to confirm the leak-free system. The AAC-EDC system was then evacuated to remove the R134a refrigerant, and nitrogen (N_2) gas was employed to ensure impurities' discharge. A vacuum pump was then connected to the service port and operated for one to 2 h to empty the AAC-EDC system. Once the leak test was done and determined that the AAC-EDC system was in good condition, the experimental method to assess its performance was conducted per the SAEJ2765 standard's regulations and recommendations.

Before the initiation of the experiment, 100 ml of 0.01 % TiO_2–SiO_2/POE nanolubricant was used to lubricate the EDC. The refrigeration system was then charged with the required quantity of R134a. The necessary amount of refrigerant, measured in grams, was then determined using a scale. After adding water to the water bath, care was taken to submerge the evaporator fully. With the aid of the water heater, the intake and output water temperatures were matched. In addition, the inlet water flow rate was maintained at 3 lpm. After completing all pre-experiment preparations, the AAC-EDC system was activated, and the initial speed was adjusted to 1200 rpm by modulating the PWM duty cycle. Before that, the frequency was set at 50 Hz. After 15 min of operation, the pressure, temperature, water mass flow rate, and power consumption were measured and recorded for the next 5 min. After that, the heater and compressor were turned off, and the data recording was terminated.

The experiment was repeated with different compressor speeds. The compressor speeds ranged between 1200 and 3840 rpm at 660 rpm intervals. After the initial refrigerant charge was completed, the steps were repeated for additional charges of 120–160 g. The

Table 3
Experimental parameters for the AAC-EDC system.

Parameters	Unit	Range
EDC compressor speed	rpm	1200 to 3840
Refrigerant charge	g	120 to 160
Volume concentration, φ	%	0 to 0.10

process was then repeated with various nanolubricant volume concentrations. The AAC-EDC system required cleaning by draining out all previously utilised nanolubricants using a refrigerant recovery unit. This step required verifying that the previous samples did not contaminate the subsequent nanolubricant sample. The parameters of the AAC-EDC system used in the experiment are listed in Table 3.

3.3. Experimental performance analysis

The vapour-compression refrigeration cycle is the primary cycle used in refrigerators, air-conditioning systems, and heat pumps. It is most suitable for describing the data analysis of the AAC-EDC system. Fig. 6 illustrates the *T-s* diagram of the ideal and actual VCR cycle. In this diagram, temperature and entropy data for the specific location were required to determine the enthalpy value of each point The diagram illustrates that the compressor's input is situated at point T_1, where the refrigerant, which is slightly superheated, enters the compressor. It is then compressed until it reaches the high pressure and high temperature state at the compressor's exit, shown as point T_2. During compression process, work (W_{in}) will be supplied to the compressor. Point T_3 denotes the location at which the high-pressure refrigerant is introduced into the condenser. Heat rejection (Q_H) causes the refrigerant to condense into a high-pressure liquid state. The fully saturated refrigerant flows into the expansion valve at point T_5 following the departure of the refrigerant in its liquid state from the condenser at point T_4. At this point, the expansion valve was compelled to enlarge the saturated liquid refrigerant into the saturated mixed refrigerant. The temperature and pressure of the refrigerant were decreased with $h_5 \sim h_6$ for the throttling operation from point T_5 to point T_6. Upon passing through the expansion valve, the refrigerant, which has been cooled, enters the evaporator, and absorbs heat (Q_L) at point T_7, causing it to transition into the vapour phase. Ultimately, the refrigerant departs from the evaporator at point T_8 and returns to the compressor's inlet at point T_1 in the form of a saturated vapour. This loop perpetuates indefinitely as the AAC-EDC system is operational. However, the current investigation primarily examined analysed the ideal parameters of the VCR cycle, with a particular emphasis on points T_1 to T_6, which correspond to the heat absorption process. The exclusion of points T_7 to T_8 in the calculation of heat absorption in the cycle by taking consideration on the following assumptions: the small pressure difference between discharge and condensation was considered insignificant, the small pressure difference between evaporator inlet and outlet was considered insignificant, and the isentropic expansion in the capillary tube was assumed to result in the same enthalpy for condensation and evaporation ($h_5 = h_6$) [55–57].

At specific points and conditions, temperature and pressure measurements concerning compressor work, heat absorption, cooling capacity, and COP are crucial. The exact value of the enthalpy point was computed using the measured temperature and pressure. This experiment collected data on temperatures and pressures using five distinct beginning refrigerant charges, five specific volume concentrations, and five different compressor speeds. It was repeated three times to guarantee each data set's precision and dependability. Before temperature and pressure measurements, the AAC-EDC was under steady-state settings, per SAE International Standard SAEJ2765 [58]. It calculated and determined the enthalpy at the point of interest by analysing the temperature and pressure. Consequently, it is possible to determine the heat absorption (q_L), compressor work (W_{in}), and performance coefficient (COP). The performance of the system was evaluated based on Equations (2)–(4).

$$q_L = h_1 - h_6 \tag{2}$$

$$W_{in} = h_2 - h_1 \tag{3}$$

$$\mathrm{COP} = \frac{Q_L}{W_{in}} = \frac{h_1 - h_6}{h_2 - h_1} \tag{4}$$

3.4. Uncertainty and consistency analysis

The current experiment used various measuring devices and sensors, including thermocouples, refrigerant gauges, flow meters, and weighing scales. Table 4 presents an inventory of the sensors and apparatus employed in the study, along with an assessment of the level of uncertainty for measured variables associated with each component. Meanwhile, the uncertainty for calculated variables is shown in Table 5. The present uncertainty analysis used a fractional uncertainty derivation to summarise the error analysis for measured and calculated variables. The measured variables are temperature, pressure and power consumption, while the calculated variables are heat absorption, compressor work and coefficient of performance (COP). In Table 4, the uncertainty for the measured variables was estimated between 0.06 % and 0.27 %. On the other hand, in Table 5, the calculated experimental parameters uncertainty was evaluated between 0.37 % and 1.37 %.

Further, the data measurement error for the AAC-EDC performance parameters was calculated using the relative standard error (RSE) method for data consistency analysis. Equation (5) was used in the investigation, where $\overline{X}$ is the mean, σ is the standard deviation, and n is the number of samples. This parameter serves as the basis for evaluating the RSE.

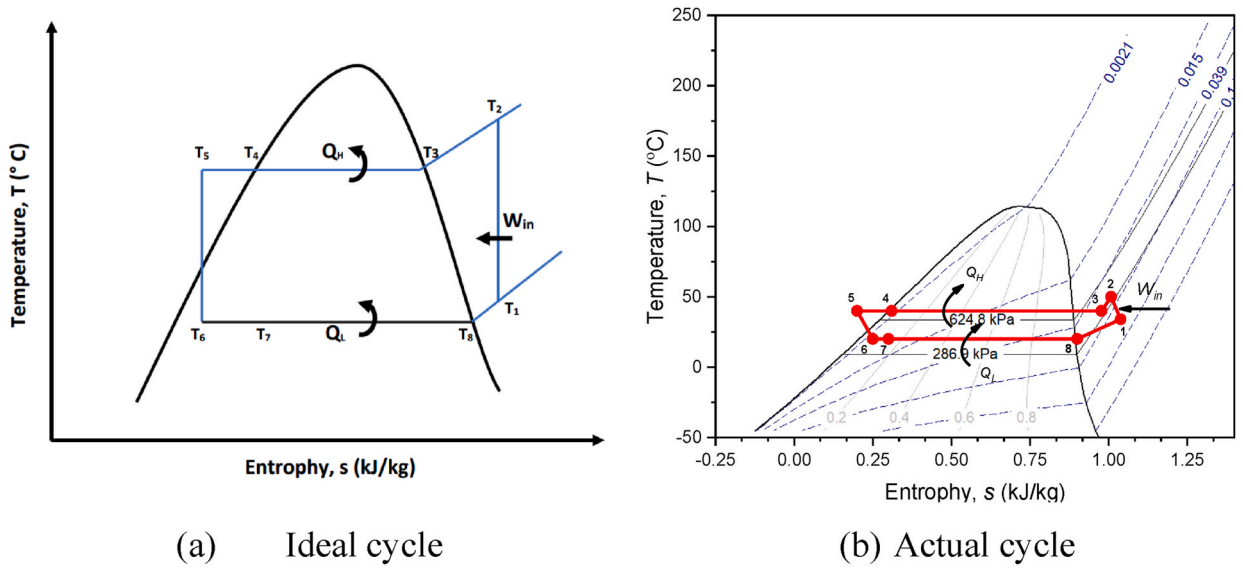

Fig. 6. The schematic of basic principle of the refrigeration system (a) Ideal cycle (b) Actual cycle.

$$RSE = \frac{S_{err}}{\overline{X}} x100\% \text{ where } S_{err} = \frac{\sigma}{\sqrt{n}} \tag{5}$$

According to the compressor's speed, Table 6 summarises the percentages of RSE for the AAC-EDC performance parameters of heat absorption, compressor work, coefficient of performance (COP), and EDC power usage. The amount of error, expressed as a percentage, is lower than 0.35 %, which is well within the range of acceptable values.

4. Results and discussion

4.1. Performance analysis at different compressor speeds

Fig. 7 illustrates the compressor work of binary TiO_2–SiO_2/POE nanolubricant and pure POE lubricants as a function of compressor speed. In particular, TiO_2–SiO_2/POE nanolubricant at 0.01 % volume concentration was compared with pure POE lubricant at various refrigerant charge initial concentrations. It was observed that the compressor work for both types of lubricants increased as the compressor speed increased, while there was no significant impact on compressor work with varying initial refrigerant charges. This trend indicates that the refrigerant charge has little effect on the compressor work, whether for POE lubricants or TiO_2–SiO_2/POE nanolubricants. However, the compressor work for TiO_2–SiO_2/POE nanolubricant was generally higher than that for pure POE lubricants, especially for initial refrigerant charges of 120 and 160 g, across all compressor speed ranges. Conversely, the compressor work for binary nanolubricant at an initial refrigerant charge of 140 g varied in response to compressor speed changes. This behaviour can be attributed to the lower superheating rate of nanolubricants, which causes them to require more work from the compressor than base lubricants [59,60].

Fig. 8 shows the EDC power consumption for TiO_2–SiO_2/POE nanolubricant at 0.01 % volume concentration. The EDC power consumption for binary nanolubricants and POE lubricants increased with increasing compressor speed. The trends for power consumption variation with compressor speed are almost identical for both lubricants. However, the refrigerant charge has an insignificant effect on the EDC power consumption for binary nanolubricants and POE lubricants. Overall, the power consumption for TiO_2–SiO_2/POE nanolubricant is slightly higher than based lubricants, especially for 120 and 160 g of initial refrigerant charge. This observation agrees with the compressor work trend in the previous figure. Under high workload conditions, the compressor tends to use more load or input power. Therefore, the findings in Figs. 7 and 8 were correlated with each other.

Fig. 9 shows the heat absorption when binary TiO_2–SiO_2/POE nanolubricant is used in the AAC-EDC system with varying compressor speeds and initial refrigerant charges. The heat absorption increased with increased compressor speed and initial refrigerant charge. Compared to pure POE lubricants, TiO_2–SiO_2/POE nanolubricant absorbed more heat in the evaporator. The maximum increment in heat absorption, up to 31.3 % higher than POE lubricants, was observed at a refrigerant charge of 160 g. On the other hand, at 120 g refrigerant charge showed the lowest increment in heat absorption compared to pure POE lubricants, with an average enhancement of 3.9 %. The observed improvement can be ascribed to the higher thermal characteristics exhibited by binary nanolubricants compared to their respective base lubricants [61].

The expansion valve discharge temperature for TiO_2–SiO_2/POE nanolubricant compared to POE lubricants at different refrigerant charges and various compressor speeds is depicted in Fig. 10. The discharge temperature from the expansion valve was seen to decrease to a particular level as the compressor's speed was increased. Similarly, the temperature also reduced with the increased initial refrigerant charge. The TiO_2–SiO_2/POE nanolubricant achieved a minimum expansion valve discharge temperature of 11.07 °C

Table 4
Summary of the uncertainty for the measured variables.

Experimental sensors and measuring equipment				
Sensors/Equipment	Measured Range	Least division	Uncertainty (%)	
			Min	Max
K-type thermocouple, °C	316 to 677	±1.5	0.38	0.27
Refrigerant gauge, kPa	8.1 to 50.0	±0.5	0.07	0.16
Power clamp, W	120 to 170	±0.1	0.06	0.08

Table 5
Summary of the uncertainty for the calculated parameters.

Calculated variables	Uncertainty (%)
Heat absorption	0.49–1.29
Compressor Work	0.37–0.47
Coefficient of Performance (COP)	0.61–1.37

Table 6
The consistency values of the experimental data at different compressor speed.

Speed, N	Percentage relative standard error, RSE (%)			
rpm	Q_L	W_{in}	COP	P_{USAGE}
1200	0.16	0.11	0.28	0.35
1860	0.08	0.12	0.23	0.15
2520	0.07	0.14	0.12	0.09
3180	0.05	0.09	0.04	0.05
3840	0.06	0.08	0.14	0.14

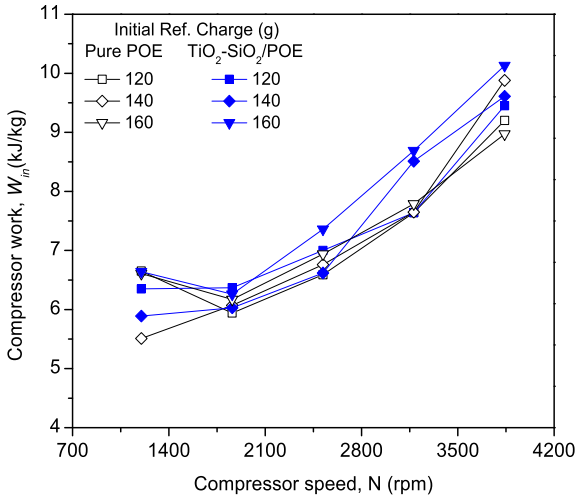

Fig. 7. Compressor work of TiO_2–SiO_2/POE at different compressor speeds.

when the initial refrigerant charge was 160 g. This finding occurred at a maximum compressor speed of 3840 rpm. In general, utilising TiO_2–SiO_2/POE nanolubricants demonstrates greater efficacy than POE lubricants in reducing the discharge temperature of the expansion valve. This outcome holds true for refrigerant charges of 140 and 160 g and various compressor speed conditions. But, at an initial refrigerant charge of 120 g, the temperature decrement of the expansion valve discharge was slightly lower than that of pure POE lubricant. The present finding for expansion valve discharge temperature is compatible with the previous outcome in Fig. 9 for heat absorption. The high heat absorption by the evaporator represents more heat loss from the refrigerant-nanolubricant mixture. Subsequently, the discharge temperature from the expansion valve for binary nanolubricants was reduced significantly compared to POE lubricants.

The COP performance of the AAC-EDC system utilising binary TiO_2–SiO_2/POE nanolubricant at different compressor speeds was compared to that of pure POE lubricants, and the results were presented in Fig. 11. It was observed that the COP for both types of

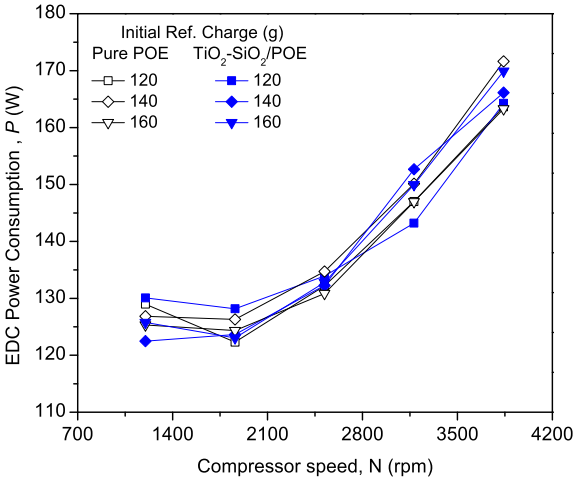

Fig. 8. EDC power consumption of TiO_2–SiO_2/POE at different compressor speeds.

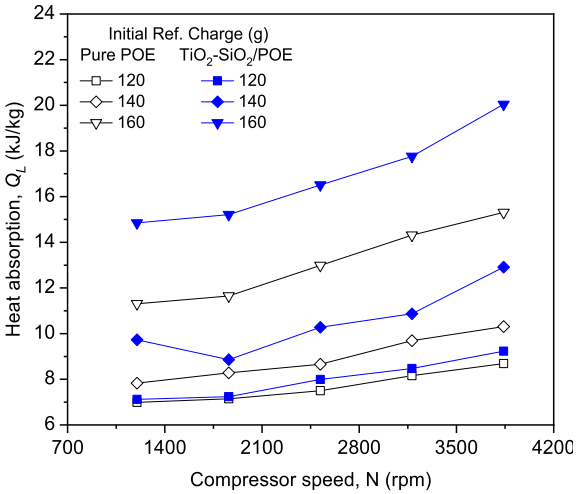

Fig. 9. Heat absorption of TiO_2–SiO_2/POE nanolubricant at different compressor speeds.

lubricants increased with an increment of refrigerant charge. However, the COP initially rose with the compressor speed before decreasing, which was attributed to the impact of heat absorption and compressor work. Furthermore, it may be associated with the likelihood of refrigerant gas leakage during the compression process and the reduction in compressor mass flow rate [62]. The COP for TiO_2–SiO_2/POE nanolubricant was higher than that of the pure POE lubricants, especially at an initial refrigerant charge of 160 g. On the other hand, the increase in the COP for the binary nanolubricant at 120 g of refrigerant charge was insignificant. The nanolubricant achieved the highest COP value of 2.43 at 160 g of refrigerant charge and 1860 rpm speed. Therefore, binary TiO_2–SiO_2/POE nanolubricant performed better in the AAC-EDC system than pure POE lubricant.

4.2. Performance analysis at different volume concentrations

A summary of the compressor work for binary nanolubricants at various volume concentrations is shown in Fig. 12. The AAC-EDC system using binary TiO_2–SiO_2/POE nanolubricants was operated with higher compressor work than POE lubricants and recorded for all volume concentrations. Concurrently, the compressor work of binary nanolubricants with 0.03 % volume concentration always shows lower values than the compressor work compared to other volume concentrations. This finding relates to the rheological behaviour and tribological performance of binary nanolubricants [63]. An increase in compressor effort caused by the inclusion of nanoparticles contributes to the rise in COP. Increased heat transfers due to increased surface area led to a surge in compressor work. The nanoparticles are distributed uniformly at the molecular level of the lubricant. Consequently, the surface area for heat transfer is enhanced. This behaviour is one of the primary causes of the rise in thermal conductivity and heat transmission.

The EDC power consumption at various volume concentrations for binary nanolubricants is also depicted in Fig. 12. The EDC power consumption for binary TiO_2–SiO_2/POE nanolubricants was increased higher than POE lubricant and complied for all volume concentrations. These results were related to the pumping force, heat generation and energy loss within the compressor, and well-

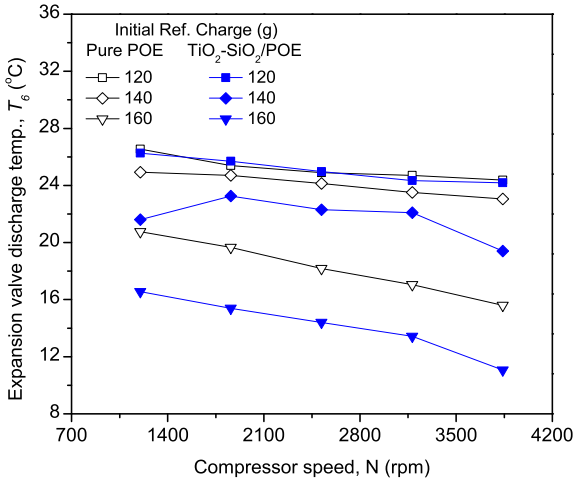

Fig. 10. Expansion valve discharge temperature of TiO_2–SiO_2/POE nanolubricant at different compressor speeds.

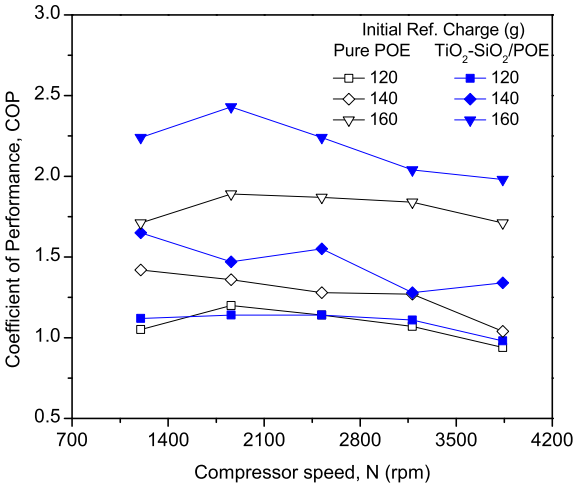

Fig. 11. Coefficient of performance of TiO_2–SiO_2/POE nanolubricant at different compressor speeds.

enhanced heat transfer capabilities of nanolubricants. In addition, the combined impacts of increasing heat absorption were much more than the increased compression work, increasing the compressor's power consumption. Subsequently, the increment of EDC power consumption happens accordingly with the increment of compressor work. To summarise the evaluation of compressor performance, it was determined that TiO_2–SiO_2/POE nanolubricant, specifically at a volume concentration of 0.03 %, outperforms POE lubricants by exhibiting lower compressor work and EDC power consumption.

Fig. 13 depicts the summary of heat absorption for binary TiO_2–SiO_2/POE nanolubricants at various concentrations. From the figure, it was observed that binary nanolubricants at all volume concentrations absorbed more heat at a significantly higher rate than pure POE lubricants, with an increment of 30.89 % and up to 42.46 %. The heat absorption of binary nanolubricants ranged between 19.67 and 22.08 kJ/kg, higher than the heat absorption of POE lubricants, which was 15.31 kJ/kg. Therefore, the binary nanolubricants in the AAC- EDC system execute with significant heat absorption improvement over POE lubricants for all volume concentrations. However, the initial refrigerant charge variation must influence the best heat absorption performance. Even though the binary nanolubricants perform well regarding heat absorption, the compressor's work performance must be scrutinised. It is meaningless to claim that nanolubricants, particularly binary TiO_2–SiO_2/POE lubricants, achieve good performance solely based on heat absorption if the work done by the compressor is significantly greater than that of pure POE lubricant. Therefore, COP analysis is required to conclude the present binary nanolubricants' overall performance by considering both components of compressor work and heat absorption.

Also in Fig. 13, different volume concentrations of TiO_2–SiO_2/POE nanolubricants provide different cooling capacities. The cooling capacity for the present binary nanolubricants is significantly higher than that of pure POE lubricants, except for the 0.1 % volume concentration. Using binary nanolubricants at a volume concentration of 0.03 %, the AAC with EDC system has 50 % greater cooling capacity than the pure lubricant. Generally, the cooling capacity of the nanolubricants increases with volume concentration up to 0.03

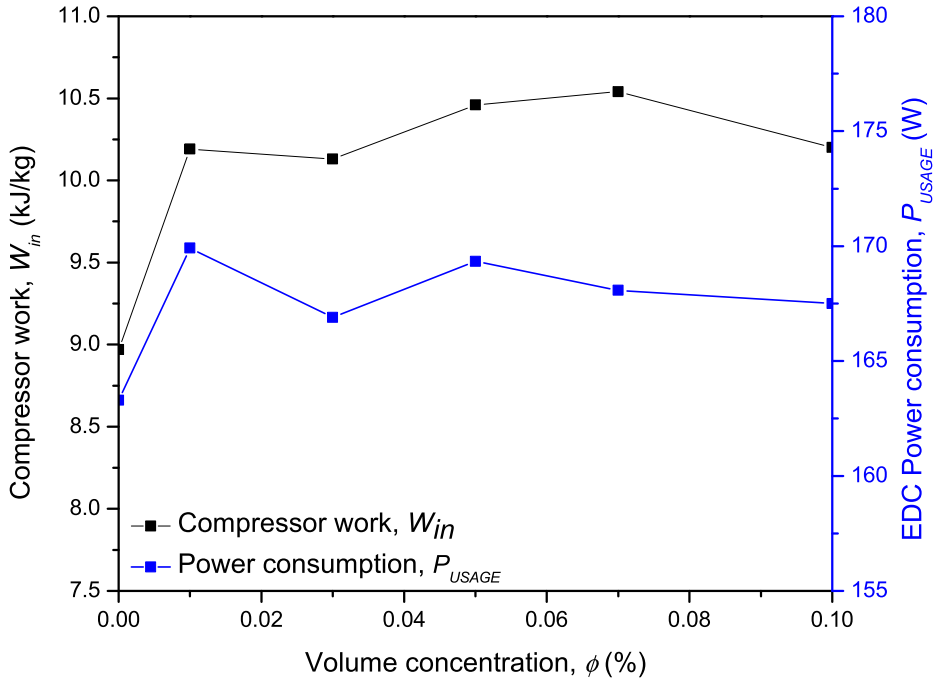

Fig. 12. Compressor work and EDC power consumption of binary nanolubricants at different volume concentrations.

% and then decreases beyond that concentration. The reduction in cooling capacity can be attributed to the increased compressor discharge pressure, which leads to a decrease in the mass flowrate of refrigerant. In addition, the enhanced cooling capacity is a result of the elevated thermal conductivity of the binary nanoparticles, leading to an increase in the amount of heat absorbed by the system [64]. To summarise the cooling performance evaluation, the nanolubricants significantly improve the heat absorption by the evaporator, with TiO_2–SiO_2/POE binary nanolubricant providing the best cooling capacity at a volume concentration of 0.03 %.

Fig. 14 illustrates the impact of binary nanolubricants on the suction and discharge temperature of the compressor. The discharge temperature for pure POE lubricant is 46.1 °C, while the suction temperature is 33.2 °C. The temperature of the discharged temperature of compressor increases with the highest increase occurring at a volume concentration of 0.03 %, resulting in a 10.41 % increment. The lowest temperature increase occurs at 7.59 % for both 0.08 % and 0.10 % volume concentrations. At a volume concentration of 0.08 %, the compressor's suction temperature decreases by a maximum of 4.5 %. The highest increase in suction temperature, on the other hand, is observed at a volume concentration of 0.9 %, with an increment of 0.03 %. Overall trend is linear due to compressor effect at the inlet and outlet at all concentration. Elevated discharge temperature leads to increased condensing temperature and decreased evaporating temperatures.

Fig. 15 presents the expansion valve discharge temperature at varying volume concentrations for binary TiO_2–SiO_2/POE nanolubricants. The figure shows that binary nanolubricants drastically reduced expansion valve discharge temperature compared to pure POE lubricants, decreasing between 24.4 % and 51.6 %. Furthermore, the temperature declined as the volume concentration increased, with similar temperature variation for all nanolubricants. The binary TiO_2–SiO_2/POE nanolubricant achieved the lowest expansion valve discharge temperature of 7.55 °C at 0.07 % volume concentration. Overall, TiO_2–SiO_2/POE nanolubricants outperform POE lubricants in reducing expansion valve discharge temperature, resulting in lower temperatures at all volume concentrations. Hence, employing binary nanolubricants in the AAC-EDC system reduces the expansion valve discharge temperature.

Fig. 15 also summarises the variation of COP for the nanolubricants. The graph demonstrates that the COP of the binary nanolubricants consistently outperformed the POE lubricants at all studied volume concentrations in this investigation. Notably, the highest COP increment of up to 23.39 % was observed at a volume concentration of 0.03 %. Thus, the findings demonstrate that the nanolubricants performed remarkably well in terms of COP and exhibit significant potential for practical implementation in the AAC-EDC system. The improved performance of COP can be related to the more outstanding heat absorption capabilities and reduced compressor work of the nanolubricants. As the availability of greater energy levels increases, the rate at which heat is transferred also increases, leading to an overall COP rise in the system [65]. In addition, the inclusion of binary nanolubricants enhances the COP and cooling capacity by diminishing the energy consumption of the compressor in comparison to the nanolubricant-free system [66]. This trend is supported by a research study conducted by Babarinde and Madyira [67] and Babarinde et al. [68].

The mean improvement of system parameters at various volume concentrations is outlined in Table 7. From the table, binary nanolubricants with a volume concentration of 0.03 % exhibit the smallest average improvement in compressor work and power consumption, with enhancements of 12.93 % and 2.20 % respectively, compared to other volume concentrations. Furthermore, binary TiO_2–SiO_2/POE nanolubricants exhibited a considerably higher heat absorption rate compared to pure POE lubricants, with an

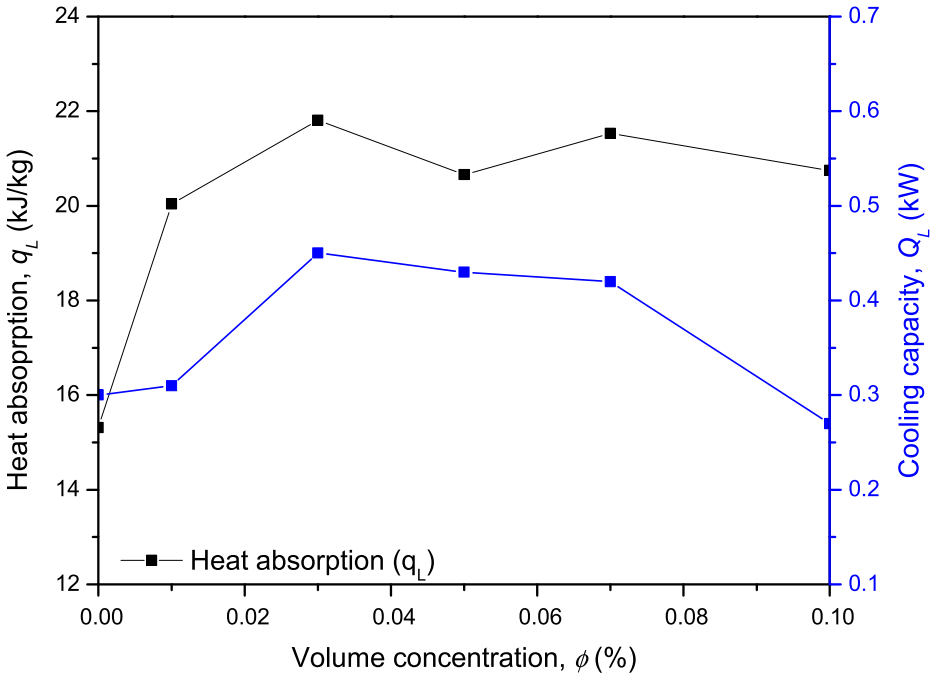

Fig. 13. Heat absorption and cooling capacity of binary nanolubricants at different volume concentrations.

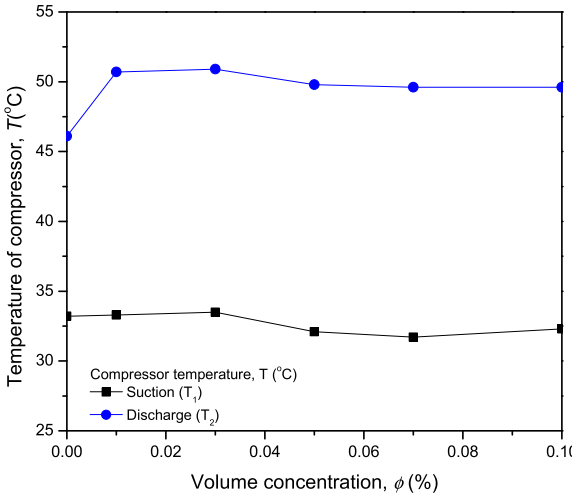

Fig. 14. Discharge and suction temperature of the compressor of binary nanolubricants at different volume concentrations.

increase of up to 42.46 % across all volume concentrations. The AAC with EDC system exhibits a cooling capacity that is 50 % higher than the pure lubricant, except for when the volume concentration is 0.1 %. An increase in the COP of up to 23.39 % was observed when the volume concentration was 0.03 %.

5. Conclusions

A comprehensive evaluation of the AAC-EDC system was carried out using TiO_2–SiO_2/POE nanolubricants. The formulation and characterisation of the binary nanolubricants were investigated to ensure the system's stability. Subsequently, the experimental effort focused on evaluating the performance of the AAC-EDC system using binary nanolubricants in terms of heat absorption, compressor work, cooling capacity, COP, and EDC power consumption. The following conclusions were drawn regarding the use of binary nanolubricants.

i. A volume concentration of 0.03 % provided the best performance with the lowest compressor work and minimum EDC power consumption.

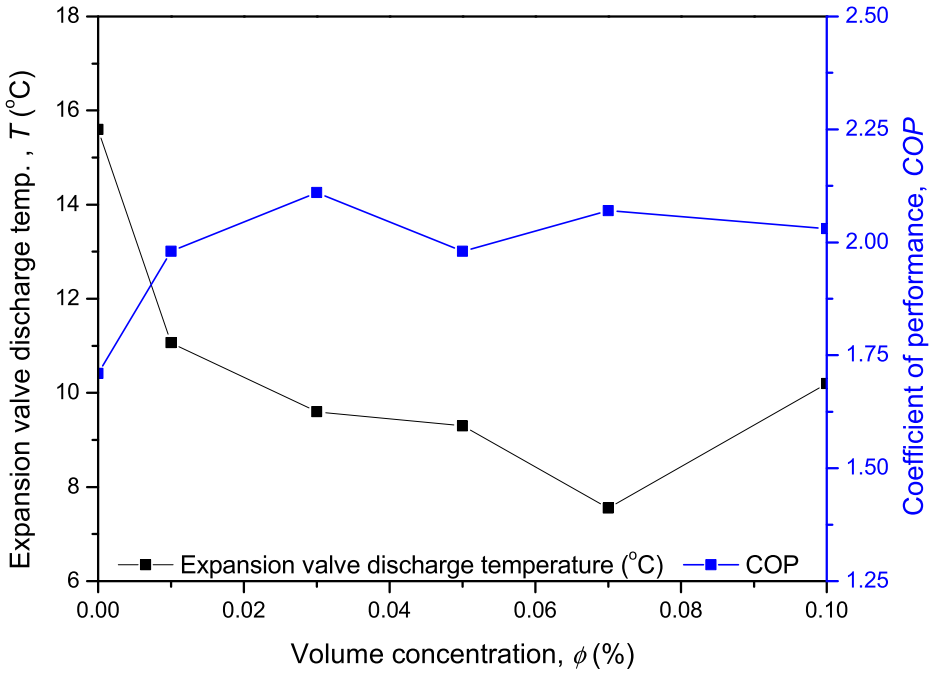

Fig. 15. Expansion valve discharge temperature and coefficient of performance of binary nanolubricants at different volume concentrations.

Table 7
Average enhancement for AAC system performance of TiO_2–SiO_2/POE binary nanolubricants at different volume concentrations.

Volume Concentration, φ (%)	Average enhancement (%)				
	Compressor work	Heat absorption	Cooling capacity	COP	Power consumption
0.01	13.60	30.89	3.33	15.79	4.06
0.03	12.93	42.46	50.00	23.39	2.20
0.05	16.61	34.94	43.33	15.79	3.71
0.07	17.50	40.63	40.00	21.05	2.93
0.10	13.71	35.53	−10.00	18.71	2.58

ii. The binary nanolubricants significantly improved heat absorption by up to 44.2 % through the evaporator of the AAC-EDC system.
iii. The binary nanolubricants exhibited exceptional performance, with a maximum increase in COP of 23.4 %.

Considering the experimental findings, the binary TiO_2–SiO_2/POE nanolubricants at a volume concentration of 0.03 % are strongly suggested for use in the AAC-EDC system, as they displayed the highest efficiency of all nanolubricants tested under various operating circumstances.

CRediT authorship contribution statement

N.N.M. Zawawi: Conceptualization, Writing – original draft. **Azmi W.H.:** Supervision, Validation, Writing – review & editing. **A. H. Hamisa:** Conceptualization, Investigation, Methodology, Writing – original draft. **Tri Yuni Hendrawati:** Formal analysis, Project administration, Resources. **A.R.M. Aminullah:** Investigation, Methodology.

Declaration of competing interest

The authors declare that they have no known competing financial interests or personal relationships that could have appeared to influence the work reported in this paper.

Data availability

No data was used for the research described in the article.

Acknowledgements

The authors appreciate the financial support provided by the Universiti Malaysia Pahang Al-Sultan Abdullah (RDU223021) under the Distinguished Research Grant, and additional financial support under the Postgraduate Research grant PGRS230392. The authors further acknowledge the contributions of the research teams from the Center for Research in Advanced Fluid and Processes (Pusat Bendalir) and the Advanced Automotive Liquids Laboratory (AALL), who provided valuable insight and expertise for the current study.

References

[1] G.E. Khoury, D. Clodic, Method of test and measurements of fuel consumption due to air conditioning operation on the new prius II hybrid vehicle, Journal of Passenger Car 114 (2005) 2563–2571.
[2] I.M. Zulhilmi, P.M. Heerwan, S.M. Asyraf, I.M. Sollehudin, I.M. Ishak, Experimental study on the effect of emergency braking without anti-lock braking system to vehicle dynamics behaviour, Int. J. Automot. Mech. Eng. 17 (2020) 7832–7841.
[3] M.A. Roscher, W. Leidholdt, J. Trepte, High efficiency energy management in BEV applications, Int. J. Electr. Power Energy Syst. 37 (2012) 126–130.
[4] S. Ahmadi, S.M.T. Bathaee, A.H. Hosseinpour, Improving fuel economy and performance of a fuel-cell hybrid electric vehicle (fuel-cell, battery, and ultra-capacitor) using optimized energy management strategy, Energy Convers. Manag. 160 (2018) 74–84.
[5] C. Park, H. Lee, Y. Hwang, R. Radermacher, Recent advances in vapor compression cycle technologies, Int. J. Refrig. 60 (2015) 118–134.
[6] M.F. Sukri, M.N. Musa, M.Y. Senawi, H. Nasution, Achieving a better energy-efficient automotive air-conditioning system: a review of potential technologies and strategies for vapor compression refrigeration cycle, Energy Efficiency 8 (2015) 1201–1229.
[7] A. Manoj Babu, S. Nallusamy, K. Rajan, Experimental analysis on vapour compression refrigeration system using nanolubricant with HFC-134a refrigerant, in: Nano Hybrids vol. 9, Trans Tech Publ, 2016, pp. 33–43.
[8] M.Z. Sharif, W.H. Azmi, R. Mamat, A.I.M. Shaiful, Mechanism for improvement in refrigeration system performance by using nanorefrigerants and nanolubricants – a review, Int. Commun. Heat Mass Tran. 92 (2018) 56–63.
[9] A. Senthilkumar, A. Anderson, R. Praveen, Prospective of nanolubricants and nano refrigerants on energy saving in vapour compression refrigeration system – a review, Mater. Today: Proc. 33 (2020) 886–889.
[10] R. Farrington, J. Rugh, Impact of Vehicle Air-Conditioning on Fuel Economy, Tailpipe Emissions, and Electric Vehicle Range, National Renewable Energy Lab., Golden, CO (US), 2000.
[11] S.I. Kim, G.H. Lee, J.J. Lee, J.P. Hong, Simple design approach for improving characteristics of interior permanent magnet synchronous motors for electric air-conditioner systems in HEV, Int. J. Automot. Technol. 11 (2010) 277–282.
[12] G. Guyonvarch, C. Aloup, C. Petitjean, A.D.M. De Savasse, 42 V electric air conditioning systems (EA/CS) for low emissions, architecture, comfort and safety of next generation vehicles, in: SAE Technical Paper, 2001.
[13] N. Henry, M.H.Z. Yamani, K. Sumeru, Performance study of DC compressor for automotive air conditioning system, in: Advanced Materials Research, vol. 614, Trans Tech Publ, 2013, pp. 674–677.
[14] K.D. Sendil, R. Elansezhian, Experimental study on Al_2O_3-R134a nano refrigerant in refrigeration system, International Journal of Modern Engineering Research 2 (2012) 3927–3929.
[15] K.D. Sendil, R. Elansezhian, ZnO nanorefrigerant in R152a refrigeration system for energy conservation and green environment, Front. Mech. Eng. 9 (2014) 75–80.
[16] N. Subramani, M.J. Prakash, Experimental studies on a vapour compression system using nanorefrigerants, Int. J. Eng. Sci. Technol. 3 (2011) 95–102.
[17] R.K. Sabareesh, N. Gobinath, V. Sajith, S. Das, C.B. Sobhan, Application of TiO_2 nanoparticles as a lubricant-additive for vapor compression refrigeration systems–An experimental investigation, Int. J. Refrig. 35 (2012) 1989–1996.
[18] S. Bi, K. Guo, Z. Liu, J. Wu, Performance of a domestic refrigerator using TiO_2-R600a nano-refrigerant as working fluid, Energy Convers. Manag. 52 (2011) 733–737.
[19] O.S. Ohunakin, D.S. Adelekan, T.O. Babarinde, R.O. Leramo, F.I. Abam, C.D. Diarra, Experimental investigation of TiO_2-, SiO_2-and Al_2O_3-lubricants for a domestic refrigerator system using LPG as working fluid, Appl. Therm. Eng. 127 (2017) 1469–1477.
[20] M. Xing, R. Wang, J. Yu, Application of fullerene C60 nano-oil for performance enhancement of domestic refrigerator compressors, Int. J. Refrig. 40 (2014) 398–403.
[21] N.N.M. Zawawi, W.H. Azmi, M.F. Ghazali, H.M. Ali, Performance of air-conditioning system with different nanoparticle composition ratio of hybrid nanolubricant, Micromachines 13 (2022) 1871.
[22] A.A.M. Redhwan, W.H. Azmi, M.Z. Sharif, N.N.M. Zawawi, O.W. Zulkarnain, A.R.M. Aminullah, The effect of Al_2O_3/PAG nanolubricant towards automotive air conditioning (AAC) power consumption, in: IOP Conference Series: Materials Science and Engineering, vol. 863, IOP Publishing, 2020 012056.
[23] A. Senthilkumar, A. Anderson, Experimental investigation of SiO_2 nanolubricants for R410A vapour compression refrigeration system, Mater. Today: Proc. 44 (2021) 3613–3617.
[24] A.H. Hamisa, T.M. Yusof, W.H. Azmi, R. Mamat, M.Z. Sharif, The stability of TiO_2/POE nanolubricant for automotive air-conditioning system of hybrid electric vehicles, in: IOP Conference Series: Materials Science and Engineering, vol. 863, IOP Publishing, 2020 012050.
[25] A.H. Hamisa, W.H. Azmi, T.M. Yusof, M.F. Ismail, A.I. Ramadhan, Rheological properties of TiO_2/POE nanolubricant for automotive air-conditioning system, Journal of Advanced Research in Fluid Mechanics and Thermal Sciences 90 (2022) 10–22.
[26] N.N.M. Zawawi, W.H. Azmi, M.F. Ghazali, Performance of Al_2O_3-SiO_2/PAG composite nanolubricants in automotive air-conditioning system, Appl. Therm. Eng. 204 (2022) 117998.
[27] M.Z. Sharif, W.H. Azmi, M.F. Ghazali, N.N.M. Zawawi, H.M. Ali, Viscosity and friction reduction of double-end-capped polyalkylene glycol nanolubricants for eco-friendly refrigerant, Lubricants 11 (2023) 129.
[28] R.S. Krishnan, M. Arulprakasajothi, K. Logesh, N.D. Raja, M. Rajendra, Analysis and feasibilty of nano-lubricant in vapour compression refrigeration system, Mater. Today: Proc. 5 (2018) 20580–20587.
[29] S. Bobbo, L. Fedele, M. Fabrizio, S. Barison, S. Battiston, C. Pagura, Influence of nanoparticles dispersion in POE oils on lubricity and R134a solubility, Int. J. Refrig. 33 (2010) 1180–1186.
[30] S. Narayanasarma, B.T. Kuzhiveli, Evaluation of the properties of POE/SiO_2 nanolubricant for an energy-efficient refrigeration system–An experimental assessment, Powder Technol. 356 (2019) 1029–1044.
[31] E.E. Nunez, N.G. Demas, K. Polychronopoulou, A.A. Polycarpou, Tribological study comparing PAG and POE lubricants used in air-conditioning compressors under the presence of CO_2, Tribol. Trans. 51 (2008) 790–797.
[32] A.A.M. Redhwan, W.H. Azmi, M.Z. Sharif, R. Mamat, N.N.M. Zawawi, Comparative study of thermo-physical properties of SiO_2 and Al_2O_3 nanoparticles dispersed in PAG lubricant, Appl. Therm. Eng. 116 (2017) 823–832.
[33] A.H. Hamisa, W.H. Azmi, N.N.M. Zawawi, M.Z. Sharif, A.I.M. Shaiful, Comparative study of single and composite nanolubricants in automotive air-conditioning (AAC) system performance, in: IOP Conference Series: Materials Science and Engineering, vol. 469, IOP Publishing, 2019 012044.
[34] M. Sharif, W. Azmi, A. Redhwan, R. Mamat, T. Yusof, Performance analysis of SiO2/PAG nanolubricant in automotive air conditioning system, Int. J. Refrig. 75 (2017) 204–216.
[35] A.A.M. Redhwan, W.H. Azmi, G. Najafi, M.Z. Sharif, N.N.M. Zawawi, Application of response surface methodology in optimization of automotive air-conditioning performance operating with SiO_2/PAG nanolubricant, J. Therm. Anal. Calorim. 135 (2019) 1269–1283.
[36] M.Z. Sharif, W.H. Azmi, M.F. Ghazali, N.N.M. Zawawi, H.M. Ali, Numerical and thermo-energy analysis of cycling in automotive air-conditioning operating with hybrid nanolubricants and R1234yf, Numer. Heat Tran. Part A: Applications 83 (2023) 935–957.

[37] S. Aldrich, Safety data sheet, in: Silicon Dioxide and Titanium Dioxide, 2013.
[38] W.H. Azmi, K.V. Sharma, P.K. Sarma, R. Mamat, G. Najafi, Heat transfer and friction factor of water based TiO_2 and SiO_2 nanofluids under turbulent flow in a tube, Int. Commun. Heat Mass Tran. 59 (2014) 30–38.
[39] Emkarate, RL68H, in: Typical Properties Data Sheet, Lubrizol, CPI Engineering Services, 2016.
[40] Z. Haddad, C. Abid, H.F. Oztop, A. Mataoui, A review on how the researchers prepare their nanofluids, Int. J. Therm. Sci. 76 (2014) 168–189.
[41] A.M. Abdullah, A.R. Chowdhury, Y. Yang, H. Vasquez, H.J. Moore, J.G. Parsons, K. Lozano, J.J. Gutierrez, K.S. Martirosyan, M.J. Uddin, Tailoring the viscosity of water and ethylene glycol based TiO_2 nanofluids, J. Mol. Liq. 297 (2020) 111982.
[42] M.F. Nabil, W.H. Azmi, K.A. Hamid, R. Mamat, Experimental investigation of heat transfer and friction factor of TiO_2-SiO_2 nanofluids in water:ethylene glycol mixture, Int. J. Heat Mass Tran. 124 (2018) 1361–1369.
[43] A.S. Dalkılıç, G. Yalçın, B.O. Küçükyıldırım, S. Öztuna, A. Akdoğan Eker, C. Jumpholkul, S. Nakkaew, S. Wongwises, Experimental study on the thermal conductivity of water-based CNT-SiO_2 hybrid nanofluids, Int. Commun. Heat Mass Tran. 99 (2018) 18–25.
[44] G.M. Moldoveanu, G. Huminic, A.A. Minea, A. Huminic, Experimental study on thermal conductivity of stabilized Al_2O_3 and SiO_2 nanofluids and their hybrid, Int. J. Heat Mass Tran. 127 (2018) 450–457.
[45] R.S. Kumar, T. Sharma, Stability and rheological properties of nanofluids stabilized by SiO_2 nanoparticles and SiO_2-TiO_2 nanocomposites for oilfield applications, Colloids Surf. A Physicochem. Eng. Asp. 539 (2018) 171–183.
[46] E.M. Carlisle, Silicon: an essential element for the chick, Science 178 (1972) 619–621.
[47] P.G. Jeelani, P. Mulay, R. Venkat, C. Ramalingam, Multifaceted application of silica nanoparticles, A Review, Silicon 12 (2019) 1337–1354.
[48] T.N. Hunter, E.J. Wanless, G.J. Jameson, R.J. Pugh, Non-ionic surfactant interactions with hydrophobic nanoparticles: impact on foam stability, Colloids Surf. A Physicochem. Eng. Asp. 347 (2009) 81–89.
[49] M. Schmitt, S. Limage, R. Denoyel, M. Antoni, Effect of SPAN80 on the structure of emulsified aqueous suspensions, Colloids Surf. A Physicochem. Eng. Asp. 521 (2017) 121–132.
[50] H. Tang, D. Xiang, F. Wang, J. Mao, X. Tan, Y. Wang, 5-ASA-loaded SiO_2 nanoparticles-a novel drug delivery system targeting therapy on ulcerative colitis in mice, Mol. Med. Rep. 15 (2017) 1117–1122.
[51] A.K. Tiwari, N.S. Pandya, Z. Said, H.F. Öztop, N. Abu-Hamdeh, 4S consideration (synthesis, sonication, surfactant, stability) for the thermal conductivity of CeO_2 with MWCNT and water based hybrid nanofluid: an experimental assessment, Colloids Surf. A Physicochem. Eng. Asp. 610 (2021) 125918.
[52] A.H. Hamisa, W.H. Azmi, T.M. Yusof, M.Z. Sharif, A.A. Dahlan, Development of automotive air-conditioning system test rig for hybrid electric vehicles, in: Journal of Physics: Conference Series, vol. 2000, IOP Publishing, 2021 012006.
[53] ASHRAE, Standard 41.9-2000, in: ASHRAE, 2011.
[54] SAEJ2765, SAEJ2765-Procedure for measuring system COP [coefficient of performance] of a mobile air conditioning system on a test bench, in: SAE Internationals, 2008, p. 20.
[55] M.Z. Sharif, W.H. Azmi, A.A.M. Redhwan, R. Mamat, T.M. Yusof, Performance analysis of SiO_2/PAG nanolubricant in automotive air conditioning system, Int. J. Refrig. 75 (2017) 204–216.
[56] S.S. Chauhan, Performance evaluation of ice plant operating on R134a blended with varied concentration of Al_2O_3-SiO_2/PAG composite nanolubricant by experimental approach, International Journal of Refrigeration-Revue Internationale Du Froid 113 (2020) 196–205.
[57] O.S. Ohunakin, D.S. Adelekan, T.O. Babarinde, R.O. Leramo, F.I. Abam, C.D. Diarra, Experimental investigation of TiO_2-, SiO_2- and Al_2O_3-lubricants for a domestic refrigerator system using LPG as working fluid, Appl. Therm. Eng. 127 (2017) 1469–1477.
[58] S.I.S. SAEJ2765, SAEJ2765-Procedure for measuring system COP [coefficient of performance] of a mobile air conditioning system on a test bench, in: SAE Internationals, 2008, p. 20.
[59] M.Z. Sharif, W.H. Azmi, M.F. Ghazali, N.N.M. Zawawi, H.M. Ali, Numerical and thermo-energy analysis of cycling in automotive air-conditioning operating with hybrid nanolubricants and R1234yf, Numer. Heat Tran. Part A: Applications (2022).
[60] N.N.M. Zawawi, A.H. Hamisa, W.H. Azmi, T.Y. Hendrawati, S. Safril, Performance of hybrid electric vehicle air-conditioning using SiO_2/POE nanolubricant, Case Stud. Therm. Eng. 52 (2023) 103717.
[61] N.N.M. Zawawi, W.H. Azmi, M.Z. Sharif, G. Najafi, Experimental investigation on stability and thermo-physical properties of Al_2O_3–SiO_2/PAG nanolubricants with different nanoparticle ratios, J. Therm. Anal. Calorim. 135 (2019) 1243–1255.
[62] D.F.M. Pico, L.R.R. da Silva, P.S. Schneider, E.P. Bandarra Filho, Performance evaluation of diamond nanolubricants applied to a refrigeration system, Int. J. Refrig. 100 (2019) 104–112.
[63] A.H. Hamisa, W.H. Azmi, M.F. Ismail, R.A. Rahim, H.M. Ali, Tribology performance of polyol-ester based TiO_2, SiO_2, and their hybrid nanolubricants, Lubricants 11 (2023) 18.
[64] T.O. Babarinde, S.A. Akinlabi, D.M. Madyira, F.M. Ekundayo, Enhancing the energy efficiency of vapour compression refrigerator system using R600a with graphene nanolubricant, Energy Rep. 6 (2020) 1–10.
[65] Z. Said, S.M. Rahman, M.A. Sohail, A.M. Bahman, M.A. Alim, S. Shaik, A.M. Radwan, I.I. El-Sharkawy, Nano-refrigerants and Nano-Lubricants in Refrigeration: Synthesis, Mechanisms, Applications, and Challenges, 2023 121211.
[66] A. Senthilkumar, P.V. Abhishek, M. Adithyan, A. Arjun, Experimental investigation of CuO/SiO_2 hybrid nano-lubricant in R600a vapour compression refrigeration system, Mater. Today: Proc. 45 (2021) 6083–6086.
[67] T.O. Babarinde, D.M. Madyira, Assessment of TiO_2, Al_2O_3, and SiO_2 nanolubricant with eco-friendly refrigerant as substitute for R134a in a vapour compression system: an experimental approach, Energy Rep. 9 (2023) 326–331.
[68] T.O. Babarinde, S.A. Akinlabi, D.M. Madyira, Experimental investigation of R600a/TiO_2/mineral oil as a drop-in replacement for R134a/POE oil in a household refrigeration system, Int. J. Ambient Energy 43 (2022) 539–545.